

Optimization of a temperature gradient-based oil spillage remediation system

Buliaminu Kareem · Sikiru Oladele Balogun

Received: 30 September 2013 / Accepted: 13 February 2014 / Published online: 30 April 2014
© The Author(s) 2014. This article is published with open access at Springerlink.com

Abstract This paper examines the deficiencies of existing oil spillage remediating techniques and their inabilities to achieve optimal result at maximum efficiency. The development of alternative strategy for remediating oil spillage is an idea conceived from a natural phenomenon based on obvious physical changes between oil and water at lower temperature. The technique involves extensive studies of the physical, chemical and thermodynamic properties of water and hydrocarbons as well as oceans and characteristics of oceans as it is affected by temperature change, climatic condition, heat gradient, salinity, wind speed, and heat stratification. The paper also exploited critical analysis of the thermodynamics of heat transfer between two objects in constant contact as well as the existing oil spillage remediating techniques or devices for sea and land pollution. The new device was designed to generate high quality crude oil continuously from crude oil/water mixture optimally when the operational conditions are followed strictly. The step by step derivation of equation for the quantity of recovered oil from the empirical data through graphical analyses is a real representation of the conditions for effective operation of the machine in an oceanic environment. The new technique has shown a very high efficiency in quality oil separation and remediation process for a short run as well as optimal efficiency close to one hundred percent for a long run. The results achieved in the operation of the new system are well appreciable when compared with the existing remediating techniques,

although, it may be necessary to use an intermediary wave neutralization system in a rough oceanic environment to improve the oil quality and maximize efficiency.

Keywords Oil spillage · Development · Heat gradient · Remediation · Strategy and thermodynamics

Abbreviations

DCHD	Discharged
OCC	Oceanic cooling chamber
RCC	Rapid cooling chamber
RVD	Recovered
SC	Separation chamber
TGBOSRM	Temperature gradient-based oil spillage remediating machine

Introduction

Crude oil is a vital element in the world economy and Nigeria is one of the oil production nations in the world. It plays a very important role in the energy sector to the extent that an alternative replacement is proved to be abortive because it is naturally endowed and abundant in nature. The consequences of oil spillage on the seas and lands during dredging and transportation activities by oil companies are serious challenges to the world. An oil spillage is the release of a liquid petroleum hydrocarbon into the environment due to human activities, and is a form of pollution [1]. Crude oils are basically categorized as paraffins, naphthenes, aromatics depending on their hydrocarbon chains. They could also be classified as paraffin base or asphalt base depending on residue fraction of the crude oil [2]. The physical and chemical characteristics

B. Kareem (✉) · S. O. Balogun
Mechanical Engineering Department, Federal University of
Technology, P.M.B. 704, Akure, Ondo State 34001, Nigeria
e-mail: karbil2002@yahoo.com

S. O. Balogun
e-mail: gatewaypilot2012@yahoo.com

of crude oils determine their hazardous impacts on the environment. The physical characteristics include density, specific gravity, viscosity, pour point, surface tension, flash point, and emulsification. The chemical characteristics are boiling points, relative solubility, and aromatic content [3].

The existing techniques for oil spillage remediation could be categorized as biological, chemical, and mechanical methods. Bioremediation is a popular method of remediating seas and lands through the use of biological agents called microbes. The technique is further categorized into phytoremediation, mycoremediation, phytoextraction, phytostabilization, phytotransformation, bioaugmentation, bioslurp, etc. [4].

Phytoremediation is the remediation process achieved through cultivation of plants which have the natural tendency of absorbing hydrocarbon in their upper part when planted on a polluted or contaminated soil. These plants are regularly harvested and replanted until the hydrocarbon in the contaminated soil is reduced to the acceptable level. Mycoremediation is the remediation through the introduction of fungi called mycelia which has the natural ability of decomposing hydrocarbon chains [5]. Phytoextraction is a form of phytoremediation process involving the use of plants such as algae to remove contaminants from the soil in the form of plant biomass. In addition, phytotransformation is a process of soil remediation through transformation of xenobiotic substances by certain plants such as cannabis to non harmful compound by increasing their polarity [6].

Bioaugmentation is another bioremediation process which involves the introduction of inoculants to increase reactive enzymes in the contaminated area to speed up remediation process. Furthermore, bioslurping involves mechanical pumping of contaminated ground water to the surface for treatment [7]. Bioremediation has also gone to the level of genetic engineering whereby genes which are capable of remediating a particular containment are introduced at the site to spur the already naturally existing microbes in the contaminated area into action. Bioremediation process, though, is efficient and effective but has a marked disadvantage of long period of manifestation. It is mostly applicable in the lands or marshed areas.

The chemical techniques of cleaning up hydrocarbon include controlled burning [8] and dispersant method. Burning could also be referred to as combustion and could be categorized as complete or incomplete combustion depending on the outcome of the reaction [9, 10].¹ These

¹ SL Ross Environment Research Ltd, DF Dickins Associate Ltd and Alaska Clean Sea [9] jointly embarked on the experiments to determine the performance efficiencies of insitu burning of spilled oil on the sea and frazil ice. The experiment was successful but was not environmental friendly and only applicable in a remote and isolated areas because of heavy emission of poisonous carbon monoxide to the atmosphere.

processes are cheap but their negative effects on the people and surrounding atmosphere are enormous. Dispersant method is the use of chemical reaction to convert insoluble hydrocarbon into soluble hydrocarbon to facilitate its precipitation or disappearance from the surface of water [11, 12].² Dispersants could be applied in the forms of plasticizer [13], flocculants and deflocculants [14], detergent [15], surfactants [16] and solubilizers [17]. This method has been criticized for increasing toxicity of seabed, killing of fish eggs and other aquatic organisms.

Dredging is a mechanical means of evacuating sediments from the bottom of seas. The method is viable but under strict regulations in the United State of American because of several negative effects associated with the process. Some of the hazardous effects include damaging of the natural aquatic environment, exposure of dangerous contaminants or toxic substance at the bottom of sea etc. [18]. In addition, skimmer is another mechanical means of reducing effects of oil spillage and has numerous industrial applications. The disadvantage of skimmer is its inability to directly filter oil from the water. The admixture of oil and water collected from the sea will still be channeled through other devices to further separate oil from water and this actually reduces the efficiency of the device [19, 20]. In the case of drum or disc skimmer, the device picks only oil from the surface of the sea but the process is very slow. It is also well applicable in oil spillage situation [21].³

The technique for alternative strategies involves the use of heat or temperature gradient to freeze water and allow oil to separate freely and continuously without applying any external mechanical work. The newly developed machine has the advantages of regenerating pure oil continuously from oil–water mixture and it also has the tendency of removing effluent oil and hydrocarbon toxicity from the seabed.

Methods

The physical environment of the oceans was critically studied in relation to solar energy, ocean's wave energy and

² Trudel and Belore [12] jointly carried out the experiments to determine the performance efficiencies of dispersant in the laboratory and at sea. Though, the research was successful but the real analysis to determine the effectiveness of the process was difficult because of the problem of determining the quantity of precipitated and non precipitated spilled oil. The use of dispersant in combating oil spillage has been criticized for increasing toxicity of seabed and killing aquatic animals.

³ Broje and Keller [21] jointly carried out the experiments to determine the performance efficiencies of drum and olephelium skimmers and were able to establish that their efficiencies depend on viscosity, surface materials, speed of rotation etc. The experiment was successful but the process was characterized with slow speed of recovering of spilled oil.

patterns [22]. The wind energy determines the intensity of water waves and vertical mixing of water in the lakes. The light energy was studied with respect to the rate of transmission of solar radiation and change of water temperature. Other aspects of the ocean exploited include thermal stratification at epilimnion and hypolimnion; chemical stratification or meromix (mixolimnion, chemocline and monimolimnion), water waves, high water current and effect of salinity on water density and freezing point [23, 24]. Temperature of liquids was extensively studied in relationship with fluidity, viscosity, density, vaporization, pour point, solidification or freezing [25]. Physical and chemical properties of hydrocarbons are greatly influenced by temperature change. At higher temperature, some hydrocarbons exhibit high fluidity, low viscosity, low density, high vaporization etc., while at a lower temperature, reverse is the case. Pour point is the lowest temperature in which a liquid ceases to flow. Freezing liquid was also critically examined with respect to crystallization process, triple point of water and liquid hysteresis [26]. Rate of heat removal through flash and rapid freezing processes was studied to determine the rate of perpetual heat transfer from a constant heat generating source [27]. Density of a liquid is defined as the mass per unit volume of the material. Density of hydrocarbons was explored with relation to melting point, freezing point, vaporizations, viscosity, and specific gravity of different hydrocarbons [28, 29]. A liquid with low specific density tends to float on the liquid with high specific density. World Oil Spillage Modeling (WOSM) program which was developed by National Oceanic Atmospheric and Administration (NOAA) was adequately studied to determine the ratio of water–oil thickness which was capable of sustaining continuous processing with limited or negligible heat transfer. Temperature gradient was adequately explored and it is defined as a physical quality that describes in which direction and at what rate the temperature changes is most rapid around a particular location [30].

Thermodynamic heat transfer between the device and the surrounding ocean was critically examined through proper application of the first and second principles of thermodynamics [31], and other heat quantities such as thermal conductivity [32] and specific heat capacities of different materials [33], heat conductivity, convection, radiation and thermodynamic processes such as adiabatic, isochoric and isobaric. The quantity flow rate as a product of velocity and area of flow was optimally used in the graphical analysis of the empirical data and model development for both short and long run of the developed machine in laboratory (calm situation) and oceanic environment (rough situation). This was achieved through application of mathematical graphing softwares such as Microsoft Excel, MATLAB and R, Matplotlib, Graph Sight, etc.

The system will also be tested on various samples of crude oils identified in A Catalogue of Crude Oil and Product Properties [29] by comparing the crude oil characteristics such as pure point, freezing point etc. with the exit temperature of the system, T_2 to determine their suitability for the separation process.

Research concept and experimental procedure

The developed temperature gradient-based oil spillage remediating machine (TGBOSRM) was designed and fabricated based on the principles of heat energy transfer and temperature gradient formation. The machine consists of three fabricated chambers powered by cooling systems. The chambers are oceanic cooling chamber (OCC), rapid cooling chamber (RCC), and separation chamber (SC) (Fig. 1a, b). The oceanic cooling chamber (OCC) has a horizontal water way monitored with seven digital thermometers to measure temperature changes (T_1 – T_2) along the channel (Fig. 2).

The rapid cooling chamber (RCC) is equipped with fast rotating fan, cooling veins and an adjustable gate system for rapid removal of heat energy in the spill entering the machine. This enhances temperature gradient, increases stability and improves machine efficiency. Separation chamber (SC) is the point of separating the crude oil from the oil and water mixture. It is equipped with ice edge monitoring device, oil exit port, disposable stopper, digital thermometers, and cooling unit.

In the theoretical determination of the length, (L) of the water way for cooling gradient, the heat gained by water layer in the system was assumed to be proportional to the summation of the heat lost by spilled oil and surrounding ocean. In the final analysis, this is expressed as:

$$L = \sqrt{\frac{q}{1 - \eta_T}} \quad (1)$$

where system theoretical efficiency, $\eta_T = \left[\frac{C_{vw}}{C_{vo}} \right] \left[\frac{h_o}{h_w} \right] \left[\frac{\rho_o}{\rho_w} \right] \left[\frac{(T_0 - T_1)}{(T_2 - T_1)} \right]$ and constant, $q = \left(\frac{k}{\rho_w C_{vw}} \right)$. Meanwhile, C_{vo} and C_{vw} are volumetric capacities of oil and water; ρ_w and ρ_o are densities of water and oil; h_w and h_o are thicknesses of oil and water in the system; k is heat conductivity of water; and T_0 , T_1 and T_2 are temperatures of ocean, system inlet and outlet, respectively.

The theoretical equation for the length of the water way was a complete modification of the equation for heat conductivity between two plates in contact [31]

$$k = \frac{Hx}{A(T_1 - T_2)} \quad \text{or} \quad x = \frac{kA(T_1 - T_2)}{H} \quad (2)$$

where H is the heat energy; A is the area of transfer; and x is the thickness of the plate which temperature falls across

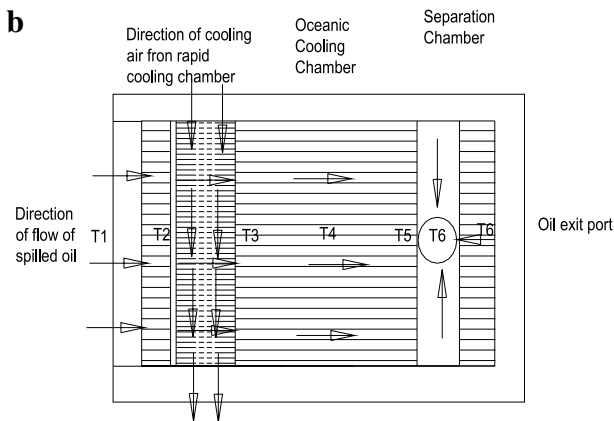
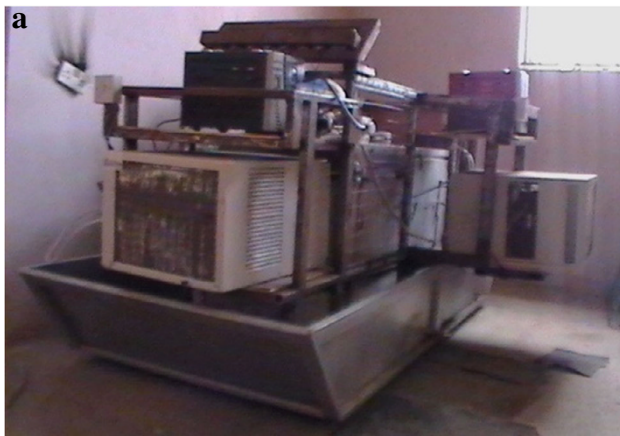


Fig. 1 a The developed temperature gradient-based oil spillage remediation machine b direction of spilled oil flow and cooling air in the developed temperature gradient oil spillage remediation machine

while T_1 , T_2 and k are as described before. In the case of the developed system, the heat transfer is between two liquids i.e., oil and water in the system and ocean. It is important to note that x in the heat transfer equation corresponds with L in the above modified equation for the developed system. Applying similarity rule to Eq. (1) and using thickness of oil (h_o) as a multiplying factor, the expression for the theoretical efficiency, η_T could be simply put as:

$$\eta_T = \frac{\text{Oil flow rate } (Q_o) - \text{Water flow rate } (Q_w)}{\text{Discharged flow rate } (Q)} \quad (3)$$

The expression for theoretical efficiency, η_T is also applicable to experimental efficiency (η_P), empirical efficiency (η_E), and simulated efficiency for oceanic wave (η_c).

Other considerations in this experiment are physical and chemical properties of the fluid specimen. These include viscosity, pour point, flash point, emulsification etc. The atmospheric conditions of the prevailing situation such as wind speed, wave condition, oceans temperature, and gate sizes were also considered. The accurate time for energy accumulation, heat dissipation, and energy rebuilding processes was equally monitored for precision analyses of the separation process. Some of the undesirable circumstances that were avoided include power fluctuation, water leakage within the system, and excessive water waves.

The spilled oil entering the machine inlet gate (Figs. 1b, 2) was subjected to a temperature gradient process which eventually enables formation of ice edge at the exit point of the water way. This phenomenon successfully impeded water flow precisely at water/oil interface and enabled the

Fig. 2 Temperature range in the developed system

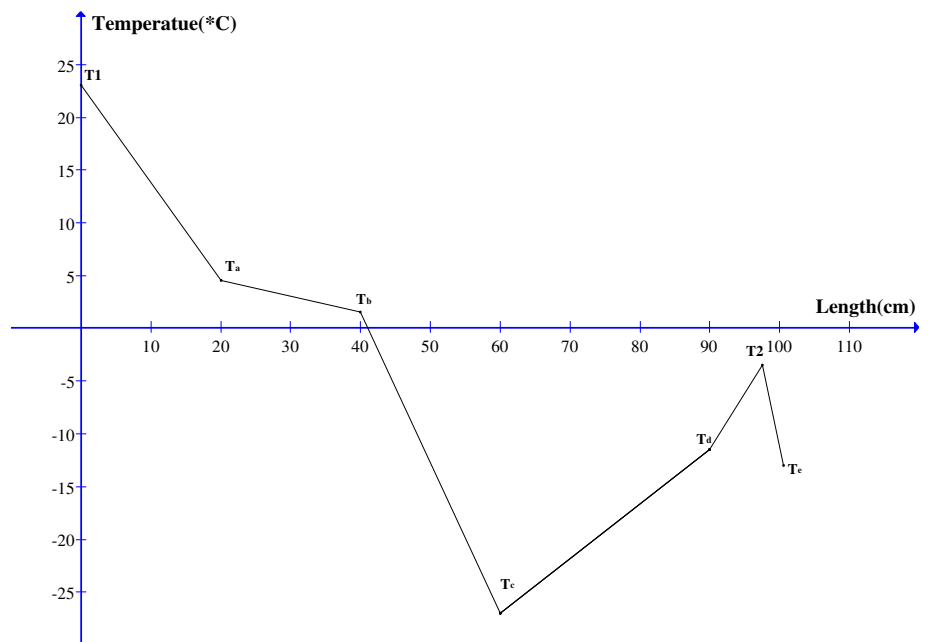


Table 1 Empirical data for recovered oil with 0.03 m gate size (size of flow inlet)

Time elapse (s)	RVD time, t (s)	Qty. DCHD, V (10^{-2} m ³)	Qty. of oil, V_o (10^{-6} m ³)	Qty. of water, V_w (10^{-6} m ³)	DCHD flow rate, Q (10^{-6} m ³ /s)	Oil flow rate, Q_o (10^{-6} m ³ /s)	% Comp. of oil	% Comp. of water	η_p (%) of TGBOSRM	Flow velocity, v (10^{-2} m/s)
13	13	28.258	25.472	2.786	2.174	1.96	90.14	9.96	88.95	4.62
26	13	29.054	28.258	0.796	2.235	2.17	97.26	2.74	97.18	4.62
40	14	29.054	27.860	1.194	2.075	1.99	95.89	4.11	95.71	4.29
56	16	28.656	27.064	1.592	1.791	1.69	94.44	5.56	94.11	3.75
71	15	27.860	27.064	0.796	1.857	1.80	97.14	2.86	97.06	4.00
88	17	29.452	27.860	1.592	1.732	1.64	94.59	5.41	94.28	3.53
109	21	28.656	28.338	0.318	1.364	1.35	98.89	1.11	98.88	2.86
127	18	29.452	29.253	0.199	1.636	1.63	99.32	0.68	99.32	3.33
152	25	29.452	29.333	0.119	1.178	1.17	99.60	0.40	99.60	2.40
182	30	27.860	27.780	0.080	0.929	0.93	99.71	0.29	99.71	2.00
209	27	29.054	28.994	0.060	1.076	1.07	99.79	0.21	99.79	2.22
242	33	31.044	30.925	0.119	0.941	0.94	99.62	0.38	99.62	1.82
282	40	29.850	29.845	0.004	0.746	0.75	99.98	0.02	99.98	1.50
334	52	31.442	31.402	0.040	0.605	0.60	99.87	0.13	99.87	1.15
384	50	30.298	30.268	0.030	0.605	0.61	99.90	0.10	99.90	1.20
436	52	29.960	29.927	0.033	0.576	0.58	99.89	0.11	99.89	1.15

Table 2 Empirical data for recovered oil with 0.035 m gate size

Elapse time (s)	RVD time, t (s)	Qty. DCHD, V (10^{-2} m)	Qty. of oil, V_o (10^{-6} m ³)	Qty. of water, V_w (10^{-6} m ³)	DCHD flow rate, Q (10^{-6} m/s)	Oil flow rate Q_o (10^{-6} m ³ /s)	% Comp. of oil	% Comp. of water	η_p (%) of TGBOSRM	Flow velocity, v (10^{-2} m/s)
9	9	27.462	24.278	3.184	3.442	2.70	88.41	11.59	86.89	6.67
19	10	29.054	27.064	1.990	2.905	2.71	93.15	6.85	92.65	6.00
28	9	28.656	26.666	1.990	3.184	2.96	93.06	6.94	92.54	6.67
37	9	30.248	30.129	0.119	3.361	3.35	99.61	0.39	99.61	6.67
46	9	29.452	29.333	0.119	3.272	3.26	99.60	0.40	99.60	6.67
56	10	26.666	26.547	0.119	2.667	2.65	99.55	0.45	99.55	6.00
76	20	30.248	30.168	0.080	1.512	1.51	99.74	0.26	99.74	3.00
88	12	29.054	28.954	0.100	2.421	2.41	99.66	0.34	99.66	5.00
115	27	28.656	28.537	0.119	2.605	1.06	99.58	0.42	99.58	2.22
132	17	29.850	29.750	0.100	1.106	1.75	99.67	0.33	99.67	3.53
144	12	31.442	31.362	0.080	2.620	2.61	99.75	0.25	99.75	5.00
157	13	29.452	29.392	0.060	2.265	2.26	99.80	0.25	99.75	4.62
172	15	29.871	29.751	0.119	1.991	1.98	99.60	0.40	99.60	4.00
189	17	30.288	29.955	0.333	1.782	1.76	98.90	1.10	98.89	3.53
209	20	31.122	31.060	0.062	1.556	1.55	99.80	0.20	99.80	3.00
241	32	28.980	28.957	0.023	0.906	0.90	99.92	0.08	99.92	1.88

recovering of high quality crude oil continuously through the exit port.

Results and discussion

The empirical data from the experimental results obtained at gate sizes of 0.030, 0.035, 0.050, and 0.055 m are

presented in Tables 1, 2, 3 and 4. In the analysis, the data related to the time elapse and quantity of discharged at the exit point of the machine were taken. These data are used to estimate quantity discharged (DCHD), V_d (m³); recovered(RVD) time, t (s); discharged flow rate, Q ; oil flow rate, Q_o (m³/s); quantity of oil, V_o (m³); quantity of water, V_w (m³); percentage composition of oil and water (%); flow velocity, v (m/s); and experimental efficiency, η_p (%).

Table 3 Empirical data for recovered oil with 0.05 m gate size

Elapse time (s)	RVD time, t (s)	Qty. DCHD, V (10^{-6} m ³)	Qty. of oil, V_o (10^{-6} m ³)	Qty. of water, V_w (10^{-6} m ³)	DCHD flow rate, Q (10^{-2} m/s)	Oil flow rate Q_o (10^{-6} m ³ /s)	% Comp. of oil	% Comp. of water	η_p (%) of TGBOSRM	Flow velocity, v (10^{-2} m/s)
2	2	29.452	24.278	5.174	14.726	12.14	82.43	17.57	78.68	30.00
5	3	29.045	24.677	4.378	9.682	8.23	84.93	15.07	82.26	20.00
8	3	31.442	28.656	2.786	10.481	9.55	91.14	8.84	90.30	20.00
11	3	31.044	30.726	0.318	10.348	10.24	98.97	1.03	98.96	20.00
17	6	28.660	27.407	1.252	4.777	4.57	95.61	4.38	95.42	10.00
25	8	31.442	31.402	0.040	3.930	3.93	99.87	0.13	99.87	7.50
38	13	30.646	30.598	0.040	2.357	2.35	99.84	0.16	99.84	4.62
53	15	29.054	28.948	0.056	1.937	1.93	99.81	0.19	99.81	4.00
73	20	29.054	29.006	0.048	1.453	1.45	99.83	0.17	99.83	3.00
95	22	30.049	30.009	0.040	1.366	1.36	99.87	0.13	99.87	2.73
115	20	28.656	28.588	0.068	1.433	1.43	99.76	0.20	99.80	3.00
139	24	31.044	31.004	0.040	1.294	1.29	99.87	0.13	99.87	2.50
163	24	30.482	30.290	0.192	1.299	1.26	99.37	0.63	99.37	2.50
189	26	31.091	31.029	0.062	1.165	1.19	99.80	0.20	99.80	2.31
214	25	29.756	29.732	0.024	1.245	1.19	99.92	0.08	99.92	2.40
244	30	29.824	29.764	0.060	0.966	0.99	99.80	0.20	99.80	2.00

Table 4 Empirical data for recovered oil with 0.055 m gate size

Elapse time (s)	RVD time, t (s)	Qty. DCHD, V (10^{-2} m ³)	Qty. of oil, V_o (10^{-6} m ³)	Qty. of water, V_w (10^{-6} m ³)	DCHD flow rate, Q (10^{-6} m ³ /s)	Oil flow rate Q_o (10^{-6} m ³ /s)	% Comp. of oil	% Comp. of water	η_p (%) of TGBOSRM	Flow velocity, v (10^{-2} m/s)
2	2	28.260	22.690	6.770	14.130	11.35	80.29	19.71	75.45	30.00
4	2	29.450	24.680	4.770	14.725	12.34	83.80	16.20	80.67	30.00
6	2	26.670	23.290	3.380	13.335	11.65	87.33	12.67	85.49	30.00
8	2	26.270	24.280	1.990	13.135	12.14	92.42	7.58	91.80	30.00
12	4	28.660	27.060	1.600	7.165	6.77	94.42	5.58	94.09	15.00
18	6	28.260	28.060	0.200	4.710	4.68	99.29	0.71	99.28	10.00
27	9	29.054	29.034	0.020	3.228	3.23	99.93	0.07	99.93	6.67
38	11	31.044	31.008	0.036	2.822	2.82	99.88	0.12	99.88	5.45
52	14	29.850	29.830	0.020	2.132	2.13	99.93	0.07	99.93	4.29
65	13	31.442	31.406	0.036	2.419	2.42	99.89	0.11	99.89	4.62
82	17	28.656	28.620	0.036	1.686	1.68	99.87	0.13	99.87	3.53
101	19	29.452	29.400	0.052	1.550	1.55	99.82	0.20	99.80	3.16
126	25	30.248	30.188	0.060	1.210	1.21	99.80	0.18	99.82	2.40
154	28	29.798	29.744	0.054	1.064	1.06	99.82	0.18	99.82	2.14
184	30	31.111	31.080	0.031	1.037	1.04	99.90	0.10	99.90	2.00
213	29	30.298	30.268	0.030	1.045	1.04	99.90	0.10	99.90	2.07

To determine the empirical efficiency of the developed machine, all the relevant properties of the test fluid must be considered to arrive at optimal model for the system. According to the conventional flow rate equation, the volumetric or discharged flow rate, Q (m³/s) is proportional to the product of flow velocity, v (m/s) and cross sectional area, A (m²) [34, 35] and it is expressed as:

$$Q = Av$$

In the developed system, the flow velocity, $v(t, g)$ is a two-dimensional quantity described in terms of elapsed time, t for a long run and gate size, g for a short run. To model $v(t, g)$ for the system, the flow velocities, $v(t)$ and $v(g)$ for various gates are graphically analyzed. The flow

Table 5 Determination of flow area (A) and oil thickness (h_o)

Gate sizes (10^{-2} m)											
Quantity of oil recovered (10^{-6} m ³ /s)				Flow area (10^{-4} m ⁴)				Flow thickness (10^{-2} m)			
3.00	3.50	5.00	5.50	3.00	3.50	5.00	5.50	3.00	3.50	5.00	5.50
2.17	3.44	14.73	14.13	0.47	0.52	0.49	0.47	3.0	3.5	5.0	5.5
2.24	2.91	9.68	14.73	0.48	0.48	0.48	0.49	0.16	0.15	0.10	0.09
2.078	3.18	10.48	13.34	0.48	0.48	0.52	0.44	0.16	0.14	0.10	0.09
1.79	3.36	10.35	13.14	0.48	0.50	0.52	0.44	0.16	0.14	0.10	0.08
1.86	3.27	4.78	7.17	0.46	0.49	0.48	0.48	0.16	0.14	0.10	0.08
1.73	2.67	3.93	4.71	0.49	0.44	0.52	0.47	0.15	0.14	0.10	0.09
1.36	1.51	2.36	3.23	0.48	0.50	0.51	0.48	0.16	0.13	0.10	0.09
1.64	2.42	1.94	2.83	0.49	0.48	0.48	0.52	0.16	0.14	0.10	0.09
1.18	2.61	1.45	2.13	0.49	1.17	0.48	0.50	0.16	0.14	0.10	0.09
0.93	1.11	1.37	2.42	0.46	0.31	0.50	0.52	0.16	0.33	0.10	0.09
1.08	2.62	1.43	1.69	0.48	0.52	0.48	0.48	0.15	0.09	0.10	0.10
0.94	2.27	1.29	1.55	0.52	0.49	0.52	0.49	0.16	0.15	0.10	0.09
0.75	1.99	1.30	1.21	0.50	0.50	0.52	0.50	0.17	0.14	0.10	0.09
0.61	1.78	1.17	1.06	0.52	0.50	0.50	0.50	0.17	0.14	0.10	0.09
0.61	1.56	1.25	1.04	0.50	0.52	0.52	0.52	0.17	0.14	0.10	0.09
0.58	0.91	0.97	1.00	0.50	0.48	0.48	0.51	0.17	0.15	0.10	0.09

velocity, $v(t)$ is the ratio of the flow length (l) to the elapse time, $t(s)$; and $v(g)$ is the flow velocity for the first sample collected at different gates representing situation similar to a large oil spillage. The flow length is the distance between the adjustable gate and exit port, and it is 0.6 m long in the fabricated machine. Using the specified value of flow length, $v(t)$ for various gate sizes can be calculated as indicated in Tables 1, 2, 3 and 4: and the graphically analysis using mathematical Graph sight gives Eq. 4 with 0.9234 regression coefficient. Likewise, flow velocity, $v(g)$ is represented by Eq. 5 with 0.67 regression coefficient.

$$v(g) = 0.107g^{3.38} \tag{4}$$

$$v(t) = 22.41t^{-0.461} \tag{5}$$

The optimized expression for the two-dimensional flow velocity using MATLAB and R is expressed in Eq. 6.

$$v(t, g) = 1.46t^{-0.231}g^{1.66} \tag{6}$$

To ascertain the area of flow as it is important in the determination of the quantity discharged, the product of oil thickness (h_o) and the gate size (g) gives the accurate value of the area of flow ($A = gh_o$). Recalling the quantity of flow in Tables 1, 2, 3 and 4 and dividing by the velocity of flow using Microsoft excel, the data for the flow area in Table 5 are achieved and further division with gate size gives the empirical data for the oil thickness on the long run.

It is observed that the oil thickness is relatively constant with time for every gate on the long run but reduces for every increase in gate size due to increase in the flow

Table 6 Determination of relationship between oil thickness and recovered time for a short run

Gate (10^{-2} m)	3.00	3.50	5.00	5.50
Oil thickness (10^{-2} m)	0.16	0.15	0.10	0.09
Recovered time (s)	13.00	10.00	3.00	2.00

velocity. This portrays the seemingly slow nature of the oil cleaning gradient when mopping up a large spill on the ocean. To determine the relationship between the oil thickness and time for a short run, the average values for the oil thickness and recovered time in Table 6 were graphically analyzed using Matplotlib to achieve the expression in Eq. 7 with a strong regression coefficient of 1.

$$t = 4153.98h_o^{3.16} \tag{7}$$

where h_o is the thickness of oil spillage on the ocean.

The flow area can be expressed as the product of oil thickness and gate size as stated earlier.

$$A = h_o g$$

Recalling the conventional flow equation and inserting the expression for the flow area:

$$Q = Vh_o g \tag{8}$$

Substituting for the flow velocity and recovered time in Eq. 8, the expression for the discharged flow rate, Q in terms of oil thickness, h_o and gate size, g_o was achieved.

$$Q = 1.46 (4153.98h_o^{3.16})^{-0.231} g^{2.66} h$$

$$Q = 0.245h_o^{0.27}g^{2.66} \tag{9}$$

where Q is the discharged flow rate (m^3/s); h_o is the oil thickness (m); and g is the gate size (m).

To determine the relationship between the discharged flow rate, Q and oil flow rate, Q_o , the empirical data for Q and Q_o for various gate sizes in the Tables 1, 2, 3, and 4 are analyzed graphically using Mathematical Graph sight and the expression in Eq. 10 with a strong regression coefficient of 0.99 was achieved.

$$Q = 1.0125Q_o^{1.034} \tag{10}$$

where Q_o is the quantity of recovered oil in m^3/s .

However, it important to note that due to the disordered nature of the graphical analysis, a scattered graph of all empirical result was plotted to determine the best relationship between the Q and Q_o . The discharged flow rate, Q in Eq. 9 is substituted in Eq. 10 and a new expression for the oil flow rate, Q_o is achieved as shown in Eq. 11.

$$Q_o = 0.254h_o^{0.261}g^{2.57} \tag{11}$$

The water flow rate, Q_w is difference between discharged flow rate, Q and oil flow rate, Q_o and it is expressed as

$$Q_w = Q - Q_o$$

Equally, the percentage composition of oil and water in the quantity discharged can be expressed as follows:

$$\% \text{ composition of oil} = 100 \left[\frac{Q_o}{Q} \right] \%$$

$$\% \text{ composition of water} = 100 - \% \text{ composition of oil}$$

The empirical efficiency of the developed temperature gradient-base oil spillage remediating machine (TGBOSRM) as reflected in the research methodology is the percentage of the ratio of difference in oil flow rate (Q_o) and water flow rate (Q_w) to oil flow rate (Q_o). This is expressed as:

$$\text{Empirical machine efficiency } (\eta_E) = 100 \left[\frac{Q_o - Q_w}{Q_o} \right]$$

Table 7 is a complete simulation of the behavior of TGBOSRM using Eqs. 9, 11 and other relevant expressions for the percentage composition of oil, water, and machine efficiency.

The least gate size for the simulated result in Table 7 is 0.01847 m width. However, other gate sizes below 0.01847 m are also effective using appropriate sizes of oil thickness.

In addition, the empirical machine efficiency could be modeled directly from the result in Table 7 with some degree of accuracy. This is done using Matplotlib for graphically analysis of oil thickness, h_o , and gate sizes, g ;

and the resulted simulated efficiency, η_m expressed in Eq. 12 has a strong correlation and regression coefficients of 0.9961 and 0.9923 when compared with empirical machine efficiency in Table 7. The F test has 0.5966 level of significance to the empirical efficiency, η_E .

$$\eta_m = 70.5g^{-0.061}h^{-0.174} \tag{12}$$

Effect of water waves on the efficiency of the machine

Water wave is generated in two ways. One is due to the gravitational attraction on the Moon, Sun and planets. They are long waves of the order of 10 m but also influenced by the water depths and geography. The Moon has twice influence on the Earth than the Sun due to its far distance from the Earth. The other wave generator is the wind due to friction and shear stress on the surface layer of the sea. Water waves are seasonal, and are classified by their wave lengths and heights [36, 37].

First consideration in the application of the developed oil spillage remediating machine in an oceanic environment was the applicable minimum angle of the prevailing wave. For high quality separation, the wave angle, θ must be within the range of the ratio of the oil thickness and gate size. This can be expressed as:

$$\theta = \tan^{-1} \frac{h_o}{g}$$

From the empirical data in Table 1, h_o and g are taken as 0.0017 and 0.030 m. Therefore, the least angle, θ of the prevailing water wave is:

$$\theta = 3.24^\circ$$

Then, subsequent increase in the wave amplitude can be taken as a multiple of the least angle.

In a simple linear wave theory as indicated by Fig. 3, the wave amplitude, A is taken to be smaller than the wave length (λ) and wave depth (d). This is referred to as small amplitude wave theory, linear wave theory, sinusoidal wave theory or airy wave. For a regular linear wave, the wave crest height (A_c) is equal to the wave trough (A_t) and is donated by the wave amplitude (A) [38].

Hence:

$$H = 2A$$

The surface elevation for a simple linear wave is expressed as:

$$\eta(x, y, t) = \frac{H}{2} \cos \theta$$

where $\theta = k(x \cos \beta + y \sin \beta) - \omega t$ and β is the direction of propagation of wave.

The surface elevation profile for a regular second order stoke wave is expressed as:

Table 7 Model test for the TGBOSRM using oil thickness and gate size as initial data input

Gate, g (10^{-2} m)	Thickness of oil, h_o (10^{-2} m)	Discharged flow rate, Q (10^{-6} m ³ /s)	Oil flow rate, Q_o (10^{-6} m ³ /s)	Water flow rate, Q_w (10^{-6} m ³ /s)	Comp. of oil (%)	Comp. of water (%)	η_E (%) of TGOSRM
1.847	0.120	0.707	0.707	0.000	99.994	0.006	99.994
1.850	0.130	0.725	0.725	0.001	99.907	0.093	99.907
2.000	0.140	0.911	0.903	0.008	99.142	0.858	99.135
3.000	0.160	2.776	2.650	0.126	95.475	4.525	95.261
3.500	0.170	4.252	4.002	0.251	94.108	5.892	93.739
4.000	0.180	6.160	5.725	0.435	92.936	7.064	92.399
5.000	0.200	11.474	10.441	1.032	91.002	8.998	90.112
5.500	0.210	14.981	13.510	1.470	90.185	9.815	89.117
6.000	0.220	19.121	17.102	2.018	89.444	10.556	88.198
10.000	0.300	80.908	68.923	11.985	85.187	14.813	82.611
15.000	0.350	248.009	203.418	44.591	82.021	17.979	78.079
20.000	0.400	552.665	441.183	111.482	79.828	20.172	74.731

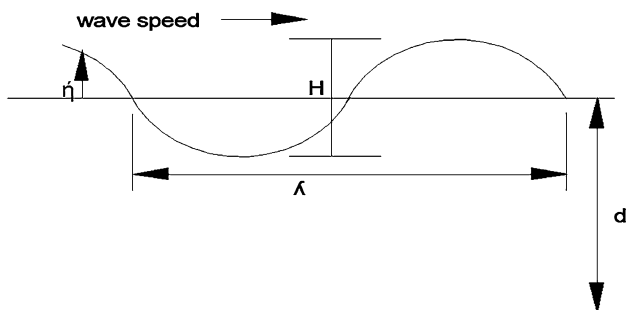


Fig. 3 A simple linear surface wave

$$\eta = \frac{H}{2} \cos\theta + \frac{\pi H^2}{8\lambda} \frac{\cosh kd}{\sinh^2 kd} (2 + \cosh^2 kd) \cos\theta$$

In deep water, the stoke second order surface elevation is:

$$\eta = \frac{H}{2} \cos\theta + \frac{AH^2}{4\lambda} \cos 2\theta$$

The phase velocity for a linear wave only depends on wave length, λ . It is expressed as:

$$c = \sqrt{\frac{gh}{2\pi} \tan h\left(\frac{2\pi d}{\lambda}\right)}$$

For deep water, the depth of a sea, $d > \lambda/2$:

$$c = \sqrt{\frac{g\lambda}{2\pi}} = \frac{g}{\omega} = \frac{gt}{2\pi}$$

For a shallow water [39]:

$$c = \sqrt{gh}$$

Recalling stokes surface elevation equation for simple linear wave:

$$\eta(x, y, t) = \frac{H}{2} \cos\theta$$

In the stoke equation, the surface wave elevation is assumed to be moving from maximum to minimum value, but in TGBOSRM, the surface elevation is assumed to be moving from the minimum to maximum value. Therefore, the cosine in stoke equation is replaced with Sine to accommodate other system parameters.

$$\eta(x, y, t) = \frac{h_o}{2} \sin\left[\frac{\theta}{n} + (n - 1)\alpha\right] \tag{13}$$

where α is the increase in wave angle due to increase in wave amplitude, while n is $1 \rightarrow \infty$ for the number of sequences for increasing the wave amplitude for a specific frequency. Alpha, α also indicates increase in the water composition in the quantity discharged due to increase in wave amplitude, while θ/n indicates gradually decreasing in the oil spread due to increase in the surface area of water as a result of increasing in water frequency and amplitude.

Substituting surface elevation in Eq. 13 for the wave amplitude, h in the phase velocity for shallow water:

$$c = \sqrt{2gh_o} \left[\frac{1}{2} \sin\left[\frac{\theta}{n} + (n - 1)\alpha\right] \right]^{1/2} \tag{14}$$

Originally, the velocity of flow equation derived from the laboratory experiment is a gravity-induced velocity which can be simply expressed as:

$$v = \sqrt{2gh_o}$$

Substituting the gravity-induced velocity of flow into Eq. 14

$$c = v \left[\frac{1}{2} \sin\left[\frac{\theta}{n} + (n - 1)\alpha\right] \right]^{1/2} \tag{15a}$$

Then, the discharged flow rate, Q_c in wavy shallow water can be expressed as:

$$Q_c = A_c$$

This can be further expanded by substituting Eq. 15a:

$$Q_c = Av \left[\frac{1}{2} \sin \left[\frac{\theta}{n} + (n-1)\alpha \right]^{1/2} \right]$$

$$Q_c = Q \left[\frac{1}{2} \sin \left[\frac{\theta}{n} + (n-1)\alpha \right]^{1/2} \right] \tag{15b}$$

where Q is the discharged flow rate in a calm situation.

Recalling the model for discharged flow rate, Q in Eq. 9 and substituting in the above equation for discharged flow rate in shallow water:

$$Q_c = 0.1225h_o^{0.27} g^{2.66} \sin \left[\frac{\theta}{n} + (n-1)\alpha \right]^{1/2} \tag{16}$$

In the same manner using the existing relationship between the discharged flow rate, Q and recovered oil, Q_o in Eq. 10, and applied to Eq. 16 putting $(n-1)\alpha$ to zero because it is the portion of discharged flow rate which represents water content due to increase in water wave amplitude.

$$Q_{co} = 0.127h_o^{0.261} g^{2.57} \sin \left[\frac{\theta}{n} \right]^{1/2} \tag{17}$$

It should also be noted that the heat transfer between the system and ocean can also cause imbalance in the efficiency of the machine. This is due to the energy coefficient resulting from the ratio of the absolute value of maximum energy rebuilding level to the absolute value of the minimum energy dissipation level. Therefore, the energy coefficient γ is introduced into Eq. 16 to achieve the new expression:

$$Q_c = 0.1225h_o^{0.27} g^{2.66} \gamma \sin \left[\frac{\theta}{n} + (n-1)\alpha \right]^{1/2} \tag{18}$$

The energy coefficient, γ determines the stability of the machine in an oceanic environment. The energy rebuilding or dissipation level is calculated from the empirical Tables 1, 2, 3, and 4 by finding the ratio of difference in the percentage composition of oil (%) and recovered time as indicated in Table 8. The positive sign in the resulted Table 8 indicates energy rebuilding level while the negative sign indicates energy dissipation level. The graphical analysis for energy levels in Table 8 is shown in Fig. 4.

$$\text{Energy rebuilding/dissipating level} = \frac{\text{Change in oil composition (\%)}}{\text{Time (s)}}$$

Table 8 Energy level in the separation process for gate 0.03 m gate

Elapse time (s)	Time (s)	Comp of oil (%)	Change in oil comp (%)	Energy rebuilding and dissipating level (s^{-1})
0	–	100	–	0
13	13	90.14	–9.86	–0.76
26	13	97.26	7.12	0.55
40	14	95.89	–1.37	–0.10
56	16	94.44	–1.45	–0.09
71	15	97.14	2.7	0.18
88	17	94.59	–2.55	–0.15
109	21	98.89	4.3	0.20
127	18	99.32	0.43	0.02
152	25	99.6	0.28	0.01
182	30	99.71	0.11	0.00
209	27	99.79	0.08	0.00
242	33	99.62	–0.17	–0.01
282	40	99.98	0.36	0.01
334	52	99.87	–0.11	0
384	50	99.9	0.03	0
436	52	99.89	–0.01	0

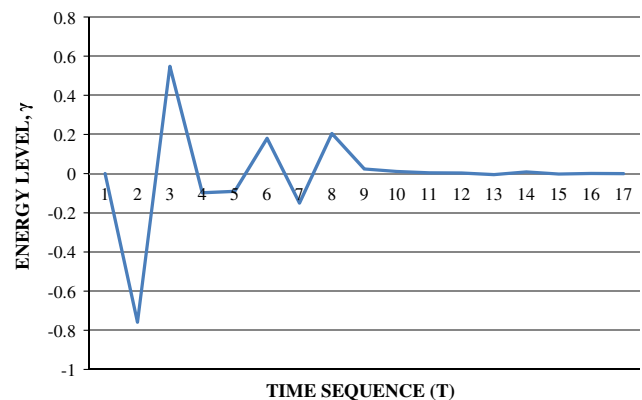


Fig. 4 Energy level of the separation process

Coefficient of energy, γ

$$= \frac{\text{Absolute value of rebuilding energy level (s}^{-1}\text{)}}{\text{Absolute value of dissipating energy level (s}^{-1}\text{)}}$$

In the above graph, the point 0.76 in energy level axis represents the coefficient of energy dissipation on a short run, and the point 0.55 in the same axis represents the coefficient of energy rebuilding in a short run. The energy coefficient is close to zero on a long run indicating the system stability in a calm situation. If the energy dissipation coefficient is continuously falling, the machine may not give a satisfactory result, and if the rate of energy rebuilding is not commensurate with energy dissipating rate, the resulted output may not be satisfactory.

Table 9 Model test for the quantity of oil recovered and machine efficiency in a wavy condition on the ocean

Number	Wave frequency, F (s^{-1})	Gate size, g (10^{-2} m)	Wave amp (10^{-2} m)	DCHD flow rate Q_c (10^{-6} m ³ /s)	Oil flow rate, Q_{co} (10^{-6} m ³ /s)	Water flow rate, Q_{cw} (10^{-6} m ³ /s)	% Comp. of oil	% Comp. of water	η_c % of TGBOSRM
1	1.00	1.847	0.17	0.02	0.02	0.00	99.09	0.91	99.08
2	1.50	1.850	0.34	0.01	0.01	0.01	57.50	42.50	26.08
3	1.70	2.000	0.51	0.02	0.01	0.02	37.73	62.27	0.00
4	1.90	2.500	0.68	0.03	0.01	0.03	27.75	72.25	0.00
5	2.00	3.000	0.85	0.06	0.01	0.05	21.88	78.12	0.00
6	2.20	3.500	1.02	0.09	0.02	0.08	18.06	81.94	0.00
7	2.40	4.000	1.19	0.12	0.02	0.12	15.38	84.62	0.00
8	2.60	4.500	1.36	0.17	0.02	0.16	13.41	86.59	0.00
9	2.80	5.000	1.53	0.22	0.03	0.21	11.90	88.10	0.00
10	3.00	5.500	1.70	0.28	0.03	0.26	10.71	89.29	0.00
11	3.20	6.000	1.87	0.35	0.03	0.32	9.75	90.25	0.00
12	3.40	6.500	2.04	0.42	0.04	0.39	8.96	91.04	0.00
13	3.60	7.000	2.21	0.50	0.04	0.46	8.30	91.70	0.00
14	3.80	7.500	2.38	0.59	0.05	0.54	7.74	92.26	0.00
15	4.00	8.000	2.55	0.69	0.05	0.63	7.26	92.74	0.00

$$\gamma = \frac{0.55}{0.76} = 0.724$$

In a wave situation, the energy dissipation coefficient may be aggravated by the wave frequency, f and coefficient of heat conductivity, k of the ocean water. For the ratio of energy coefficient and the product of water frequency, f and coefficient of heat conductivity, k for water equal one taken the coefficient of heat conductivity for water to be 0.58 at a frequency of one cycle per second, the model for the quantity discharged can further be modified as follows:

$$Q_c = 0.098h_o^{0.27} g^{2.66} \left(\frac{\gamma}{fk}\right) \sin\left[\frac{\theta}{n} + (n-1)\alpha\right]^{1/2} \quad (19)$$

Recalling Eq. 17 and applying the parameters for the energy coefficient, heat conductivity and water frequency, the equation for the quantity of recovered oil can be modified as:

$$Q_{co} = 0.1016h_o^{0.261} g^{2.57} \left(\frac{\gamma}{fk}\right) \sin\left[\frac{\theta}{n}\right]^{1/2} \quad (20)$$

Assuming that increase in wave angle, α due to increase in wave amplitude is equal to the wave angle, θ for calm situation, then the above model could be computed for various frequencies, gate sizes, and oil thickness. Meanwhile, the effect of wave amplitude on the temperature gradient along the water channel should be considered. Therefore, the maximal wave amplitude should be within one-third of the water thickness, h_w to sustain the system stability. From the laboratory experiment, water thickness was 3 cm; therefore, the maximal permissible wave amplitude was 1 cm high (Table 9).

In the graphical analysis in Fig. 5, the simulated efficiency (η_c) of the machine is greatly hampered by the oceanic waves. As the wave frequency and amplitude increase, the efficiency of the system decreases due to short time lag to replace lost energy. In addition, increase in wave amplitude gradually alters the temperature gradient zone along the water channel, thereby increasing the heat gained from the oceanic surrounding. This confirms that the system energy must be conserved by allowing a minimal allowable water wave to enter the system or by emplacing an intermediary system which is capable of neutralizing or reducing the frequency and amplitude of the water wave to achieve maximum efficiency.

Conclusions

TGBOSRM is a new device designed based on obvious physical change between oil and water at a lower temperature. The technique is successful and the oil recovered from oil–water mixture is very impressive. The pertinent question is the ability of the ice edge to withstand a separation process for a long time. The answer to this was discovered after the system was shutdown. In the separation chamber, there was a thick white shinning semi-solid layer covering and insulating the ice edge form being dissolved by the discharge from the machine. This showed that as the oil was flowing over the ice edge, there was a formation of an incomplete emulsified semi-solid thick skin layer which insulated and fortified the ice edge to perform the task. Another important point to note in this experiment is that the system was allowed to work properly

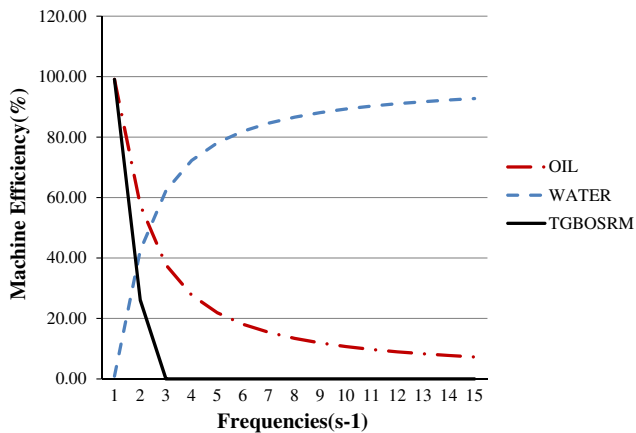


Fig. 5 Graphical analyses of recovered oil, water composition, and machine efficiency at different wave frequencies in an oceanic environment

for some minutes to enable the formation of the insulated layer. This enables effective operation and consistency in data collection for a long period of time. In addition, the quantities of recovered oil in the discharge and machine efficiency are improving towards 100 % on the long run. This is a validation of the theoretical design concept, which assumes the machine efficiency to be closed to 100 %.

It is also confirmed that the developed system can deal with 86 samples of crude oil out of 166 identified in A Catalogue of Crude Oil and Product Properties. This was achieved using $-10\text{ }^{\circ}\text{C}$ as the benchmark for pour points for suitable crude samples; between 0 and $-9.9\text{ }^{\circ}\text{C}$ for likely suitable crude oils; and above $0\text{ }^{\circ}\text{C}$ for unsuitable oils. This gave at least 58 % viability of the equipment to remediate different grades of crude oils.

Acknowledgments P.B. Mogaji, S.O. Abadariki and T.M. Adamolekun are acknowledged for their assistance during the preliminary experimentation of the system.

Conflict of interest The author declares that there is no competing interest.

Author's contributions BK carried out the experimental design, data analysis, and performance optimization of the oil spillage remediation system, participated in the construction of the system, and drafted the manuscript. SOB participated in oil spill remediation survey, construction and analysis of the remediation system. All Authors read and approved the final manuscript.

Author's information Dr. B. Kareem, Principal Investigator and an Associate Professor of Mechanical Engineering (Production and Industrial Engineering). Department of Mechanical Engineering, Federal University of Technology, Akure, E-mail: karbil2002@yahoo.com; bkareem@futa.edu.ng. Engr. S.O. Balogun, Investigator and a PhD Research Student, Department of Mechanical Engineering, Federal University of Technology, Akure, E-mail: gatewaypilot2012@yahoo.com.

Open Access This article is distributed under the terms of the Creative Commons Attribution License which permits any use, distribution, and reproduction in any medium, provided the original author(s) and the source are credited.

References

- Robertson S.B., Steen A., Skewes D., Pavia R., Walker A.H.: Marine oil spill response options. The manual, In: Proceedings of International Oil Spill Conference. American Petroleum Institute Publication no. 4651, Washington, DC (1997)
- Fiske, R.P.: US Navy ship salvage manual vol. 6 oil spill response. <http://www.supsal.org/vol%206.pdf> Ch. 2, pp. 4–7 (1991). Accessed 23 March 2011
- ExxonMobil oil spill response manual. http://www.crrc.unh.edu/dwg/exxon_oil_spill_response_field_manual.pdf Ch. 4, pp. 1–10 (2008). Accessed 12 Feb 2012
- USEPA: Factsheet on bioremediation in oil spill response (2012). <http://home.eng.iastate.edu/tge/ce421-521/thehawkenator-pres.pdf>. Accessed 2 March 2014
- Miller, R.: Phytoremediation, Technology Overview Report, Ground-Water Remediation Technologies Analysis Center, Pittsburgh, PA vol. 3 (1996)
- Bioaugmentation. <http://www.en.wikipedia.org/wiki/Bioaugmentation> (2011). Accessed 2 April 2011
- Vroblesky, D., Nietch, C., Morris, J.: Chlorinated Ethenes from groundwater in tree trunks. Environ. Sci. Technol. **33**(3), 510–515 (1998). doi:10.1021/es980848b. Accessed 12 Feb 2011
- International Spill Control Organization (ISCO) Oil spill solution: Controlled burning. http://www.oilspillsolution.org/Controlled_burning.htm (2010). Accessed 5 April 2011
- SL Ross Environment Research Ltd, DF Dickins Associate Ltd and Alaska Clean Sea.: Final report: test to determine the limit to insitu burning of thin oil slicks in broken ice. http://www.Siross.ca/publication/amop/2013-ISB-Broken_ice.pdf (2003). Accessed 5 April 2011
- International Spill Control Organization (ISCO): Controlled Burning. http://www.oilspillsolution.org/Controlled_burning.htm (2010). Accessed 5 April 2011
- National Oceanic and Atmospheric Administration (NOAA): Dispersants: A Guided Tour: PART Five. Retrieved from http://response.restoration.noaa.gov/topic_subtopic_entry.php?RECORD_K (2008). Accessed 10 April 2011
- Trudel, K., Belore, R.: Final report: Correlation of Ohmsett dispersant tests with at-sea trials, supplementary tests. <http://www.bsee.gov/Research-and-Training/Technology-Assessment-and-Research/tarproject/500-599/526AA.aspx> (2005). Accessed 12 April 2011
- Cadogan, D.F., Howick, C.J.: Plasticizers, Ullmann's Encyclopedia of Industrial Chemistry. Wiley-VCH, Weinheim. <http://www.en.wikipedia.org/wiki/Plasticizer> (2000). Accessed 23 April 2011
- Chaala, A., Benallal, B., Hachelef, S.: Investigation on the flocculation of asphaltenes and the colloidal stability of the crude oil fraction. Can. J. Chem. Eng. **72**, 1036–1041 (1994)
- Choi, H.M., Cloud, R.M.: Natural sorbents in oil spill cleanup. Environmental Science Technology. Retrieved from <http://pubs.acs.org/doi/abs/10.1021/es00028a016> (1992). Accessed 27 April 2011
- Reznik, G.O., Vishwanath, P., Pynn, M.A., Sitnik, J.M., Todd, J.J., Wu, J., Jiang, Y., Keenan, B.G.: Use of sustainable chemistry to acyl amino acid surfactant. Appl. Microbiol. Biotechnol. **5**, 1387–1397. <http://www.ncbi.nlm.nih.gov/pubmed/20094712> (2010). Accessed 27 April 2011



17. Jain, A., Ran, Y., Yalkowsky, S.: (2004): Effect of pH-Sodium Lauryl Sulfate Combination on Solubilization of PG-300995 (an Anti-HIV Agent): a technical note. *AAPS Pharm. Sci. Tech.* **45**(1) <http://www.ncbi.nlm.nih.gov/pmc/articles/PMC2750268/>. Accessed 1 March 2014
18. Sarkar, S., Bose, N., Sarkar, M., Walker, D.: Concept of a mathematical model for prediction of major design parameters of a submersible dredger/miner. 3rd Indian National Conference on Harbour and Ocean Engineering, National Institute of Oceanography, Dona Paula, India (2004). http://drs.nio.org/past_events/inchoe/inchoe_contents.jsp. Accessed 1 March 2014
19. Schulze, R.: Oil spill response performance review of skimmers. ASTM Manual Series MNL 34. West Conshohocken, PA, pp 151. http://astm.org/DIGITAL_LIBRARY/index.html (1998). Accessed 2 March 2014
20. Clauss, G.F., Kühnlein, W.L., Härtel, M.: Hydrodynamic Optimization of Selected Oil Skimming Systems, Mariglobe'93, Bremen, Germany (1993)
21. Broje, V., Keller, A.A.: Optimization of Oleophilic skimmer recovery surface, field testing at ohmstett facility. <http://www2.bren.ucsb.edu/~keller/paper/FinalReportmms2.pdf> (2006). Accessed 13 May 2011
22. Lorenz, E.N.: The nature and theory of the general circulation of atmosphere, World Meteorological Organization. Publication no. 218, Geneva, Switzerland (1967). http://eaps4.mit.edu/research/Lorenz/The_Nature_and_Theory_WMO_1967.pdf. Accessed 2 March 2014
23. Hebert, P.D.N.: Physical environment of lakes (2007). <http://www.uoguelph.ca/~phebert/publications.htm>. Accessed 2 March 2014
24. National Snow and Ice Data Centre (NSIDC): Assessing the impact of Arctic sea ice variability on the Greenland ice sheet surface mass and energy balance. (2014) http://nsidc.org/research/projects/Stroeve_sea_ice_Greenland.html. Accessed 1 March 2014
25. Burton, W.K., Cabrera, N.: Crystal Growth and Surface Structure part 1. Discussion of the Faraday Society. doi:10.1039/DF9490500033 (1949). Accessed 10 March 2010
26. Triple point. http://www.en.wikipedia.org/wiki/Triple_Point (2011). Accessed 14 May 2011
27. National Snow and Ice Data Centre (NSIDC): Sea ice. Available from <http://nsidc.org/cryosphere/seaice/index.html> (2008). Accessed 13 May 2011
28. Density. <http://www.en.wikipedia.org/wiki/Density> (2011). Accessed 23 May 2011
29. Bobra, M.: A catalogue of crude oil and product properties. http://www.bsee.gov/research_and_Training/Technology_Assessment_and_Research/tarprojects/100-199/120BC.aspx (1990). Accessed 24 May 2012
30. Temperature Gradient. http://www.en.wikipedia.org/wiki/Temperature_Gradient (2011). Accessed 24 May 2011
31. Joel, R.: Basic Engineering Technology, 5th edn., Ch. 4, pp. 48–53 (1996)
32. List of thermal conductivities. http://www.en.wikipedia.org/wiki/List_of_thermal_Conductivities (2012). Accessed 24 May 2012
33. Heat Capacity. http://www.en.wikipedia.org/wiki/Heat_Capacity (2012). Accessed 20 June 2012
34. Leopold, L.B.: Downstream Change of Velocity in Rivers. Published by American Journal of Science, vol. 251. pp. 606–624 (1953)
35. NNPSMP: Surface Water Flow Measurement for Water Quality Monitoring Projects. Published by National Nonpoint Source Monitoring Program (2008) <http://scholar.google.com/scholar?q=NNPSMP%3A+Surface/>. Accessed 2 March 2014
36. Holmes, Patric: Professional Development Programme: Coastal Infrastructure Design, Construction and Maintenance. Department of Civil and Environment Engineering, Imperial College, England (2001)
37. Langbein, W.B., Leopold, L.B.: River Channel Bars and Dunes: Theory of Kinematic Waves. Published by United State Government Printing Office, Washington (1968). books.google.com/books?isbn=1118671562. Accessed 1 March 2014
38. Veritas, D.N.: Environmental Condition and Environmental Loads. <http://www.dnv.com> pp 25 (2010). Accessed 23 July 2012
39. Tidal Resonance. In: Hydropower, Tidal Power and Wave Power. pp. 85–89. http://en.wikipedia.org/wiki/Tidal_resonance. Accessed 23 July 2013

